Fourier Transform Infrared and Electron Spectroscopy for Chemical Analysis Studies of Block Copolymers of Styrene and Dimethylsiloxane

Xin Chen and Joseph A. Gardella, Jr.*

Department of Chemistry, State University of New York at Buffalo, Buffalo, New York 14214

Philip L. Kumler

Department of Chemistry, State University of New York College at Fredonia, Fredonia, New York 14063

Received August 27, 1991; Revised Manuscript Received August 24, 1992

ABSTRACT: The surface segregation of poly(dimethylsiloxane) (PDMS) in chloroform solution cast films of styrene and dimethylsiloxane block copolymers in AB diblock and ABA and BAB triblock types was investigated by electron spectroscopy for chemical analysis and attenuated total reflectance (ATR) FTIR. The results show that the PDMS surface segregation is mainly dependent on the architectures of the block copolymers and the PDMS block length. AB-type diblock copolymers exhibit a relatively thicker pure PDMS surface layer, and the PDMS surface segregation effects were detected up to the ATR-FTIR sampling depth. All three types of block copolymers present much higher PDMS concentrations in the outermost surface region (about 0–27 Å from the air interface) than in the bulk materials. PDMS surface segregation changes were observed for some of the block copolymers after annealing the as-cast films.

Introduction

Phase-separated morphological structures, or domain structures, exist widely in multicomponent polymeric systems such as block and graft copolymers, polymer blends, and interpenetrating polymer networks (IPN's).[1] It is well known that the domain size for block copolymers is generally smaller than that of polymer blends, because the different blocks in a chain of block copolymers are connected by covalent bonds. The architecture of block copolymers limits the very large scale phase separation that occurs in polymer blends. The microheterogeneous morphological structures of block copolymers with domain dimensions of several hundred angstroms generate many of the novel and useful mechanical and surface properties. The extent to which microphase separation occurs to form supermolecular structures depends on four inherent critical features. These are (a) compositional dissimilarity (difference in solubility parameters, or chain interactions), (b) segment molecular weight (block length), (c) crystallinity of segments,[2,3] and (d) molecular architecture.[4] The morphology of block copolymers also depends on the way in which the materials are formed. For example, different morphologies can result when they are solution cast from different solvents.[5]

Bulk morphological structures have been widely investigated by means of transmission electron microscopy (TEM) and scanning electron microscopy (SEM).[6-8] Detailed surface morphological studies on block copolymers became possible only in recent years due to the newly developed surface analysis techniques, such as electron spectroscopy for chemical analysis (ESCA) (or X-ray photoelectron spectroscopy (XPS)),[3,5,9,10] ion scattering spectroscopy (ISS),[11] secondary ion mass spectroscopy (SIMS),[12] neutron reflectivity (NR),[13] forward recoil spectrometry (FRES),[14,15] and small-angle X-ray scattering (SAXS).[16] These techniques, coupled with contact angle measurements (Zisman plot)[5] and attenuated total reflectance (ATR) FTIR,[3,17,18] provide information from varying surface thicknesses, ranging from the top few angstroms (ISS, SIMS, and Zisman plot), to 20–100 Å (ESCA), to a few micrometers (ATR–FTIR), and make depth profiles of block copolymers practical.

Clark et al.[5] studied (by ESCA and contact angle measurements) the surface morphology of AB-type diblock polystyrene–poly(dimethylsiloxane) (PS–PDMS) copolymer films cast from different solvents. Their results showed that the immediate air side surface, as measured by means of the contact angle, consisted of an essentially pure PDMS component for as-cast films. The as-cast films were prepared by using solvents which were good for both the PS block and the PDMS block. However, the topmost layer of pure PDMS in the films with a low PDMS bulk concentration (41 wt %) was calculated to be much thinner than that of the films with a higher PDMS bulk concentration (77 wt %) on the basis of the electron escape depths in ESCA. No systematic studies of the effects of block length and architecture of block copolymers on surface morphology have been reported.

Schmitt et al.[3] investigated the effect of crystallinity of block copolymers on surface morphology by using ESCA and ATR-FTIR. Poly((tetramethyl-*p*-silylphenylene)-siloxane)–poly(dimethylsiloxane) multiblock copolymers having a high degree of crystallinity (90/10 and 80/20 wt % ratio of crystalline to amorphous) showed a higher concentration of the amorphous component in the surface region than that in the bulk. Gardella et al.[11] and McGrath et al.[19] have also shown surface enrichment of the lower surface energy component in block copolymers of bisphenol-A-polycarbonate (BPAC) and PDMS by ISS and ESCA. The results revealed that nearly pure PDMS covered the immediate air side surface region (3–5 Å) of the block copolymer samples if the PDMS bulk concentration in the copolymers was higher than 50 wt %. The degree of PDMS surface enrichment is much greater in the top 5-Å surface range (ISS sampling region) than in the top 50-Å surface range (ESCA sampling region).

ESCA studies[20,21] of both blends and block copolymers of polystyrene (PS) and poly(ethylene oxide) (PEO) showed that the lower surface energy component PS was present in higher concentrations in the surface region than in the bulk for both the block copolymers and the blends.

0024-9297/92/2225-6621$03.00/0

Table I
Architectures and Molecular Weights of PS–PDMS Block Copolymers

sample	type	A block (PS)	B block (PDMS)	wt % B	copolymer M_n
1	AB	27 000	94 000	77.5	121 000
2	AB	16 600	38 700	70	55 300
3	AB	70 000	99 000	58.5	169 000
4	ABA	2 × 8600	33 100	65.5	50 000
5	ABA	2 × 12 900	94 200	78.5	120 000
6	ABA	2 × 12 500	56 000	69.1	81 000
7	ABA	2 × 11 250	67 500	75	90 000
8	BAB	6600	2 × 13 200	80	33 000
9	BAB	9090	2 × 1 520	25	12 120

Secondary ion mass spectroscopy (SIMS), along with a sputter depth profiling technique, has been used to investigate the surface-induced orientation of symmetric diblock copolymers of styrene and methyl methacrylate.[12] The films of the diblock copolymer exhibited a periodic lamellar microdomain morphology oriented parallel to the surface at the thermodynamic equilibrium conditions, while the as-cast films of the copolymer from toluene exhibited no morphological orientation with respect to the surface.

The effect of block length on the surface excess of the low surface energy component in AB-type block copolymers was studied by Green et al.[10] The surface excess (ψ_1) of PS in a PS–PMMA (poly(methylmethacrylate)) symmetric diblock copolymer was shown to be well described by the equation $\psi_1 = \alpha - \beta N^{-1/2}$, which was derived from Fredrickson's mean field theory for polymer surfaces.[22] The constants α and β are related to the difference between the interactions of the two different blocks at the surface and those in the bulk, and also to the surface energy differences between the two components. This approach could be helpful in predicting the design of surface properties with specific block lengths.

In this paper we present a systematic investigation of PDMS segregation in the surface and near surface regions (from the air interface to the sampling depths of ESCA or ATR-FTIR) of PS–PDMS block copolymers with different PDMS block chain lengths and architectures. Depth profiles of the PDMS concentration (which is defined as the DMS molar fraction) obtained from ESCA and ATR-FTIR measurements provide the possibility for detailed studies of the surface morphology. Along with TEM studies of the block copolymers, a quantitative approach will be discussed in the companion paper[23] according to the results we present here.

Experimental Section

Sample Preparation. Polystyrene (PS, M_w = 280 000) was purchased from Aldrich Chemical Co., Inc., and poly(dimethylsiloxane), or PDMS, was purchased from Scientific Polymer Products, Inc. The PDMS was secondary standard (M_w = 1 010 000 and M_n = 180 000). The PDMS sheets (NHLBI-DTB primary reference material) used for ESCA and ATR-FTIR calibrations were purchased from Thoratec Laboratories Corp. (Berkeley, CA). Block copolymers of styrene and dimethylsiloxane in AB diblock, ABA triblock, and BAB triblock types were provided by Dr. Dale J. Meier of Michigan Molecular Institute. Their architecture and structure data are shown in Table I. All polymers were used as received. Block copolymer samples 1–3 are AB-type diblock copolymers which have one PS block (A block) chemically bonded with one PDMS block (B block). Samples 4–7 are ABA-type triblock copolymers. The last two samples (8 and 9) are BAB-type triblock copolymers. Polymer films (thicker than 100 μm) for ESCA and ATR-FTIR measurements were cast from about 1% chloroform solutions in clean Al weighing pans, allowed to air dry over night, and analyzed without any further preparation. The annealed samples were prepared from those as-cast samples by heating them for 3 days at 140 °C in a vacuum oven. The residual solvent in the polymer films could be monitored by the detection of chlorine by ESCA. No solvent could be detected in the films within the detection limits of ESCA (less than 1 at. %). For transmission (TX) FTIR experiments, 1–3 wt % polymer solutions in chloroform were deposited directly onto KBr plates which were then air dried over night. The thickness of the films was controlled so that the IR absorbance was between 0.3 and 1.0 in the range between 700 and 800 cm^{-1}. All ESCA, TX-FTIR, and ATR-FTIR results were averaged from the measurements of at least four separately prepared samples to ensure reproducibility. The air side of the polymer films was measured by both ESCA and ATR-FTIR.

Instrumentation. The angle-dependent ESCA experiments were performed on a Perkin-Elmer Physical Electronics Model 5300 ESCA using a hemispherical analyzer. Mg $K\alpha_{1,2}$ X-rays, from a dual anode source, were used as the excitation source. The source was operated at 300 W, 15.0 kV, and 20 mA. The base pressure was maintained at $\leq 3.0 \times 10^{-9}$ Torr. A pass energy of 17.9 eV was employed for all high-resolution angle-dependent acquisitions. Three take-off angles of 15°, 45°, and 90° led to sampling depths for ESCA experiments of 27, 73, and 103 Å,[9] respectively. Care was taken to check X-ray radiation damage on the polymer sample surface. During times twice as long as that requested for the actual overall ESCA analysis, the atomic ratios of carbon, silicon, and oxygen of several selected PS–PDMS block copolymer samples remained the same within the range of ESCA measurement error; this means that no significant radiation degradation could be detected. All data manipulation (peak area calculation, baseline subtraction) was accomplished using a Perkin-Elmer 7500 computer running PHI ESCA version 2.0 software.

Both TX-FTIR and ATR-FTIR experiments were performed on a Mattson Polaris FTIR spectrometer with a DTGS detector at a resolution of 4 cm^{-1}. For collections of TX-FTIR and ATR-FTIR spectra, 16 and 32 scans were run, respectively. Being mounted on a Harrick TPMRA attachment, a Harrick parallelogram Ge prism (50 × 10 × 3 mm) with a 45° face cut was used as the internal reflectance element for all ATR-FTIR collections. The depth of penetration (d_p) in the polymer films for the ATR-FTIR experiments was estimated to be 0.8–1.0 μm,[24] which led to a sampling depth (d_s, which is defined as $d_s = 3d_p$) of 2.4–3.0 μm from the air surface for the IR absorption bands between 700 and 800 cm^{-1}.

Calibration and Calculations

ESCA Calculations. Carbon to silicon atomic ratios in the surface and near surface regions (from the air interface to the ESCA sampling depths) were calulated from the measurements of carbon 1s (binding energy 285 eV) peak areas and silicon 2p (binding energy 103 eV) peak areas. According to the structures of the repeat units of PS (containing eight C atoms in each repeat unit) and PDMS (containing two C atoms and one Si atom in each repeat unit) segments, the DMS molar fraction is given by the equation

$$\mathrm{C/Si} = [2X + 8(1 - X)]/X \qquad (1)$$

where C/Si is the atomic ratio of carbon to silicon of the polymer film surface as measured by ESCA and X is the surface DMS molar fraction of the samples.

FTIR Calculations and Calibration. Quantitative calculations of the DMS molar fraction from ATR-FTIR measurements should be based on calibration. TX-FTIR measurements, given in Table II, of all of the nine block copolymer samples were done for the purpose of obtaining a calibration of ATR-FTIR measurements to the PDMS surface concentration of the block copolymers. Figure 1 shows TX-FTIR spectra of PS and PDMS homopolymers and a PS–PDMS block copolymer comprised of about 75% wt/wt PDMS in the range of 650–1300 cm^{-1}. An ATR-FTIR spectrum of the PS–PDMS block copolymer is also shown in this figure. PS has a very strong absorption

Table II
TX-FTIR Measurements of PS–PDMS Block Copolymers

sample	A_{700}/A_{800}	DMS molar fraction in the bulk[a]	sample	A_{700}/A_{800}	DMS molar fraction in the bulk[a]
1	0.239 ± 0.020	0.829	6	0.398 ± 0.017	0.759
2	0.376 ● 0.019	0.766	7	0.369 ● 0.032	0.808
3	0.320 ± 0.045	0.664	8	0.299 ± 0.031	0.849
4	0.499 ● 0.065	0.727	9	1.294 ± 0.080	0.319
5	0.273 ● 0.032	0.837			

[a] DMS molar fractions in the bulk were calculated from the PDMS weight percent given in Table I.

peak at 700 cm^{-1} while PDMS has a very strong absorption peak at 800 cm^{-1}. These two peaks in the PS–PDMS block copolymers are well separated but close enough to avoid a significant difference in the sampling depths, which are proportional to the wave length of the incident light. The molar absorptivity of PS at 800 cm^{-1} is zero, but that of PDMS at 700 cm^{-1} is not zero. Beer's law for a two-component system could be applied to the block copolymer samples at the wavenumbers of 700 and 800 cm^{-1}, leading to the following equations:[25]

$$A_{\lambda 1} = (\epsilon_{11}C_1 + \epsilon_{21}C_2)b \quad (2)$$

$$A_{\lambda 2} = (\epsilon_{12}C_1 + \epsilon_{22}C_2)b \quad (3)$$

where $A_{\lambda 1}$ and $A_{\lambda 2}$ are the total absorbances of the two-component (the PS segment is component 1, and the PDMS segment is component 2) samples at the two wavenumbers, namely, 700 cm^{-1} for $\lambda 1$ and 800 cm^{-1} for $\lambda 2$. The ϵ's are the molar absorptivities of the two components at the two wavenumbers, and C_1 and C_2 are the concentrations expressed in the units of moles of PS and PDMS repeat units in a unit volume, respectively. The film thickness is b. $A_{\lambda 1}$ and $A_{\lambda 2}$ were taken on the same film at the same time, so b could be canceled by taking the ratio of $A_{\lambda 1}$ to $A_{\lambda 2}$:

$$A_{\lambda 1}/A_{\lambda 2} = (\epsilon_{11}C_1 + \epsilon_{21}C_2)/(\epsilon_{12}C_1 + \epsilon_{22}C_2) \quad (4)$$

Since ϵ_{12} (the absorptivity of PS at 800 cm^{-1}) is zero, eq 4 could be simplified to

$$A_{700}/A_{800} = (\epsilon_{700}{}^{PS}C^{PS} + \epsilon_{700}{}^{PDMS}C^{PDMS})/(\epsilon_{800}{}^{PDMS}C^{PDMS}) \quad (5)$$

After the molar concentrations were converted to the DMS molar fraction, X, and the equation was rearranged, the final calbration equation reduced to

$$A_{700}/A_{800} = a(1/X - 1) + c \quad (6)$$

Both a ($a = \epsilon_{700}{}^{PS}/\epsilon_{800}{}^{PDMS}$) and c ($c = \epsilon_{700}{}^{PDMS}/\epsilon_{800}{}^{PDMS}$) are constants. Figure 2 shows the plot of A_{700}/A_{800}, measured by TX-FTIR experiments on the block copolymers, as a function of $(1/X - 1)$. The two constants a and c were determined by linear regression to be 0.520 and 0.160, respectively. The calibration equation used for ATR-FTIR measurements was finally obtained as

$$A_{700}/A_{800} = 0.520(1/X - 1) + 0.160 \quad (7)$$

According to this equation, the DMS molar fraction of the block copolymer surface can be calculated from the measurement of A_{700}/A_{800} by ATR-FTIR experiments. The wavelength correction to the absorbance measurement of ATR-FTIR is not necessary.

Results

All ESCA and ATR-FTIR data of the nine as-cast samples are summarized in Table III. The bulk DMS molar fraction data are also listed for comparison.

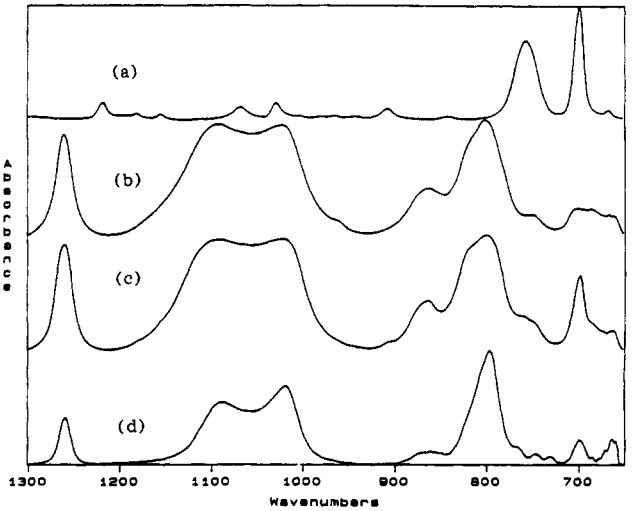

Figure 1. Transmission FTIR spectra (1300–650 cm^{-1}) of homopolymers of polystyrene (a) and poly(dimethylsiloxane) (b) and PS–PDMS block copolymer (c), sample 3. The ATR-FTIR spectrum (d) is for the same PS–PDMS block copolymer of (c). Note the difference of the absorbance ratios of the bands at 700 and 800 cm^{-1} between (c) and (d).

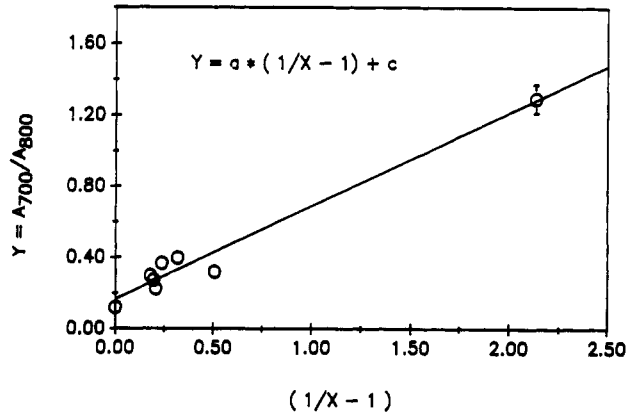

Figure 2. Calibration line of the DMS molar fraction from FTIR measurements. X is the DMS molar fraction of PS–PDMS block copolymers. Constants a and c are determined by least-squares regression to be 0.520 and 0.160, respectively.

ESCA Results from AB-Type Block Copolymers. The profiles of the DMS molar fraction versus sampling depths for the three AB-type PS–PDMS block copolymers are shown in Figure 3. Among these diblock copolymers, sample 3 has the lowest bulk PDMS concentration (DMS molar fraction is 0.664) and sample 1 has the highest bulk PDMS concentration (DMS molar fraction is 0.829). The molecular weight of sample 2 is smallest (M_n = 38 700), and that of sample 3 is the largest (M_n = 99 000). For all three AB diblock copolymers, the DMS molar fraction in the outermost 103-Å surface region is very close to unity. The results reveal that the surface region over the first 103 Å from the air interface of the diblock copolymers is composed of a nearly pure PDMS layer. These are consistent with the literature,[4] in which the data were

Table III
DMS Molar Fraction at the Surface[a] and in the Bulk of PS–PDMS Block Copolymers

sample	15° [b]	45° [b]	90° [b]	ATR-FTIR	bulk
1	0.993 ± 0.006	0.992 ± 0.008	1.005 ± 0.004	1.032 ± 0.022	0.829
2	0.996 ± 0.005	0.998 ± 0.008	1.002 ± 0.009	0.872 ± 0.015	0.766
3	0.985 ± 0.033	0.977 ± 0.018	0.971 ± 0.012	0.960 ± 0.030	0.664
4	0.868 ± 0.014	0.771 ± 0.021	0.731 ± 0.020	0.739 ± 0.097	0.727
5	0.991 ± 0.011	0.976 ± 0.007	0.977 ± 0.004	0.891 ± 0.081	0.837
6	0.961 ± 0.013	0.930 ± 0.015	0.887 ± 0.008	0.755 ± 0.070	0.759
7	0.980 ± 0.013	0.943 ± 0.027	0.930 ± 0.031	0.785 ± 0.033	0.808
8	0.948 ± 0.008	0.887 ± 0.012	0.849 ± 0.014	0.901 ± 0.038	0.849
9	0.766 ± 0.038	0.568 ± 0.013	0.508 ± 0.017	0.273 ± 0.048	0.319

[a] ESCA data of different take-off angles were calculated from C(1s)/Si(2p) atomic ratios. [b] ESCA take-off angles.

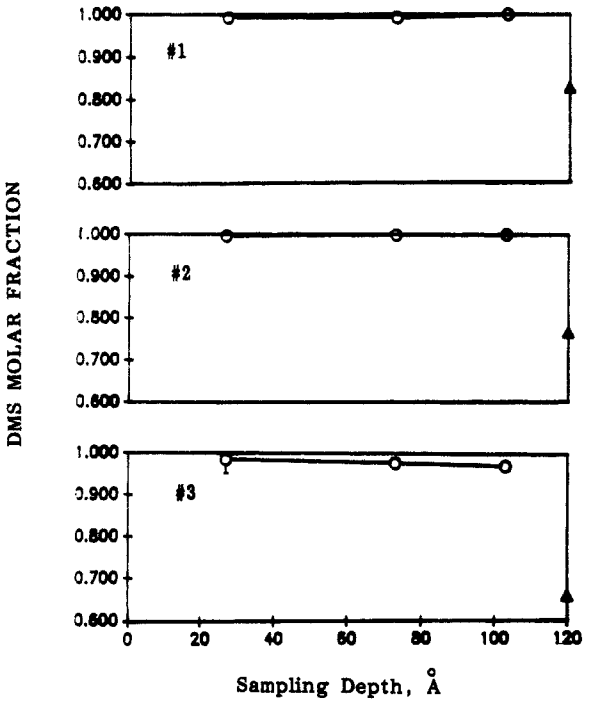

Figure 3. Depth profiles of the DMS molar fraction from ESCA for the three PS–PDMS diblock copolymers. Filled triangles are for the bulk DMS molar fractions. The profiles of samples 1–3 are arranged from top to bottom.

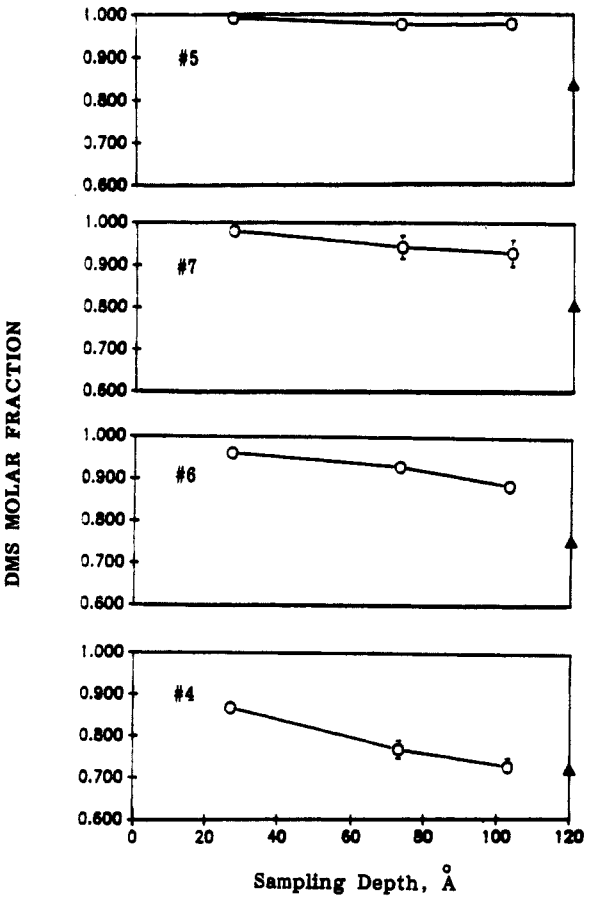

Figure 4. Depth profiles of the DMS molar fraction from ESCA for the four PS–PDMS–PS-type triblock copolymers. Filled triangles are for the bulk DMS molar fractions. The profiles of samples 4, 6, 7, and 5 are arranged from bottom to top, according to the increasing order of their PDMS block lengths.

obtained through contact angle measurements (Zisman plot), and ESCA analysis. The present results, however, show a much thicker pure PDMS outermost layer (>100 Å) than that previously estimated (>40 Å)[4] for the films of block copolymers with a comparable structure cast from chloroform solution.

ESCA Results from ABA-Type Block Copolymers. The profiles of the DMS molar fraction versus sampling depths for the four ABA-type PS–PDMS–PS triblock copolymers are presented in Figure 4. Unlike the AB-type diblock copolymers, PDMS surface concentration gradients are observed for some of the samples when the sampling depth increases. These results also show the PDMS concentration dependence in the surface regions on the PDMS block length.

The differences in bulk PDMS concentrations for the four samples (ranging from 0.727 for sample 4 to 0.837 for sample 5 in DMS molar fraction) are relatively small, compared with the differences in their PDMS block lengths, which vary from 33 100 for sample 4 to 94 200 for sample 5 in block number-average molecular weight, M_n. The four depth profiles in Figure 4 are arranged so that the PDMS block lengths of the four ABA-type samples decrease from the top to the bottom.

Sample 4 has the shortest PDMS block length (M_n = 33 100), and also the lowest DMS bulk molar fraction (0.727). The surface PDMS concentrations of this sample are much lower than those of the other three samples of the same type in each sampling region. In the sampling region of ESCA measurements at a 45° take-off angle (0–73 Å), the average PDMS concentration of this sample is close to its bulk concentration. The average PDMS concentration of this sample in the surface region measured by ESCA with a 90° take-off angle (0–103 Å) is the same as that of the bulk. Therefore, the PDMS surface segregation effect only exists in the surface region less than 103 Å for sample 4.

The PDMS surface segregation effect can be observed up to a 103-Å-thick surface region for the remaining three samples of this type. The differences in the rate of decrease of the PDMS concentration as a function of depth and PDMS block length can be seen from these depth profiles in Figure 4.

Sample 5 has the longest PDMS block (M_n = 94 200), and there is almost no decrease of PDMS surface segre-

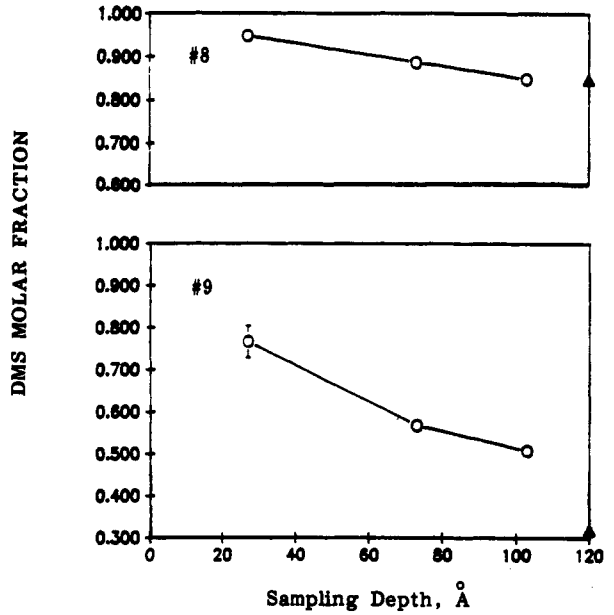

Figure 5. Depth profiles of the DMS molar fraction from ESCA for the two PDMS–PS–PDMS-type triblock copolymers. Filled triangles are for the bulk DMS molar fractions. The profiles of samples 8 and 9 are arranged from top to bottom.

gation in the three ESCA sampling depth ranges. Sample 7 has the second longest PDMS block (M_n = 67 500), and the gradient of the PDMS surface concentration is observable when the sampling depth approaches the bulk. For sample 6, with an even shorter PDMS block chain (M_n = 56 000), the surface segregation of PDMS decreases gradually as the sampling depth increases. The decrease rate of the DMS molar fraction in the surface region for sample 6 is notably larger than that for sample 7.

A comparison of the four block copolymers can also be made in the surface sampling ranges. In the outermost 27-Å-thick surface region, the DMS molar fractions of samples 5 and 7, with longer PDMS blocks, are very close to unity. It suggests that the thickness of an almost pure PDMS layer covering the surface is at least 27 Å for these two samples. Sample 6, with relatively shorter PDMS blocks, shows a small deviation of the DMS molar fraction from unity in this region (~4% mol/mol PS). Having the shortest PDMS blocks, sample 4 exhibits a much higher PS concentration (~13% mol/mol) in the same surface region. In the surface range 0–73 Å, the surface of sample 7 consists of PS (about 5%), as well as PDMS, while this layer is still covered by almost pure PDMS for sample 5, which has the longest PDMS block. Sample 6 has the same PDMS concentration in this region as sample 7, but the PDMS surface composition of samples 6 and 7 is still much larger than that of sample 4. Sample 4 has almost reached its bulk composition. When the sampling depth goes from 27 to 73 Å, the PDMS concentration of sample 4 decreases considerably faster than those of both samples 7 and 6. When the sampling depth goes from 73 to 103 Å, all the other samples still show decreases of PDMS segregation except sample 5, for which there is no substantial PS presence. In the surface region between 73 and 103 Å, sample 4 with the shortest PDMS block has reached its bulk composition, but the other three samples still exhibit considerable surface segregation of PDMS. Sample 6 with the next shortest PDMS block shows the largest decrease of PDMS segregation when the surface region measured by ESCA increases from the top 73-Å range to the top 103-Å range.

ESCA Results of BAB-Type Block Copolymers. Figure 5 shows the depth profiles of the DMS molar fraction for the two BAB-type block copolymer samples. These two samples have relatively short PDMS blocks. The M_n of each PDMS block on the copolymer chain of sample 9, for instance, is only 1520.

The surface segregation of PDMS for sample 8 gradually decreases as the sampling depth increases. In the outermost 27-Å surface region, the surface is a nearly pure PDMS layer (95% mol/mol PDMS). When the sampling depth is 103 Å, the average surface composition of the sample is the same as that of the bulk. The surface segregation effect for the sample exists only in the surface region less than 100 Å.

Sample 9 has a shorter PDMS block length and much lower PDMS bulk concentration (bulk DMS molar fraction 0.319). It exhibits a very rapid decrease in the PDMS surface concentration when the sampling depth goes from 27 to 73 Å. Then the rate of decrease slows down when the sampling depth goes from 73 to 103 Å. In the outermost 103-Å surface region, a PDMS surface segregation effect is still detectable for this sample.

ATR-FTIR Results of Block Copolymers. The sampling depth of ATR-FTIR is estimated to be between 2.4 and 3.0 μm under the experimental conditions,[24] assuming that there is no IR absorption. Since there are very strong IR absorptions by PDMS and PS in the range between 700 and 800 cm^{-1}, the sampling depth of the measurements could be much smaller. The ATR-FTIR data for the three types of block copolymers are presented in Figure 6. In Figure 6, top, the three experimental points are above the reference line, which defines equivalent bulk and surface composition. These results suggest that DMS molar fractions in the region from the air interface to the sampling depth of the ATR-FTIR measurements for all three AB-type block copolymer samples are still higher than their bulk DMS molar fractions. The effect of surface segregation of PDMS could exist up to as deep as the sampling depth of the ATR-FTIR measurements for the AB-type block copolymers with a sufficient PDMS block chain length. Furthermore, the effect of the PDMS block chain length on PDMS segregation in the sampling region can also be observed for these three AB-type diblock copolymer samples. Sample 2 with the shortest PDMS block length (M_n = 38 700) of the three samples has the lowest DMS molar fraction in the ATR-FTIR sampling region. The DMS molar fraction in this region for sample 1, which has a longer PDMS block length (M_n = 94 000), is about 1, and this means that a pure PDMS block covers the surface up to the sampling depth of the ATR-FTIR measurements. Sample 3 has nearly the same PDMS block length (M_n = 99 000) as that of sample 1, but it shows a slightly lower DMS molar fraction value (0.960) in the same surface region, possibly due to its lower PDMS bulk concentration. Even though, the DMS molar fraction in this region for sample 3 is still substantially higher than that for sample 2 with a much shorter PDMS block. The effect of the PDMS block length is a more important effect than the PDMS bulk concentration.

For ABA-type triblock copolymer samples, all four experimental points fall on the reference line across the two corners of the plot in Figure 6, middle. The compositions of the block copolymers here in the sampling range of ATR-FTIR measurements have already reached their bulk compositions. The effect of surface segregation of PDMS, which exists in shallower surface regions sampled by ESCA, has vanished. The results indirectly indicate that the sampling depth of the ATR-FTIR measurements is larger than the ESCA sampling depths.

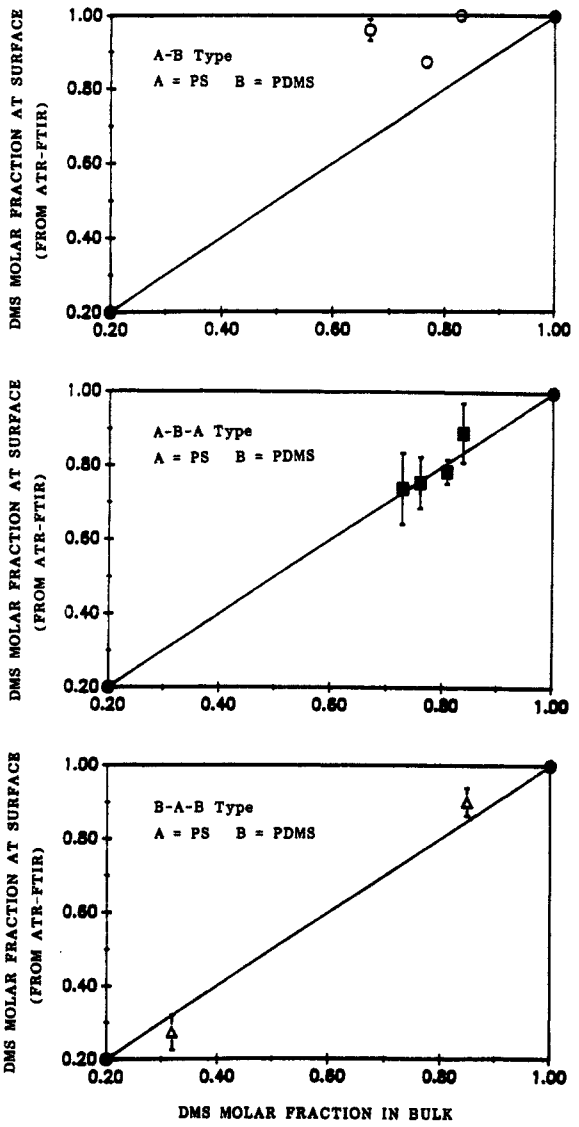

Figure 6. DMS molar fraction at the surface from ATR-FTIR versus DMS molar fraction in the bulk for the three PS–PDMS block copolymers. The plots of AB, ABA, and BAB types are arranged from top to bottom.

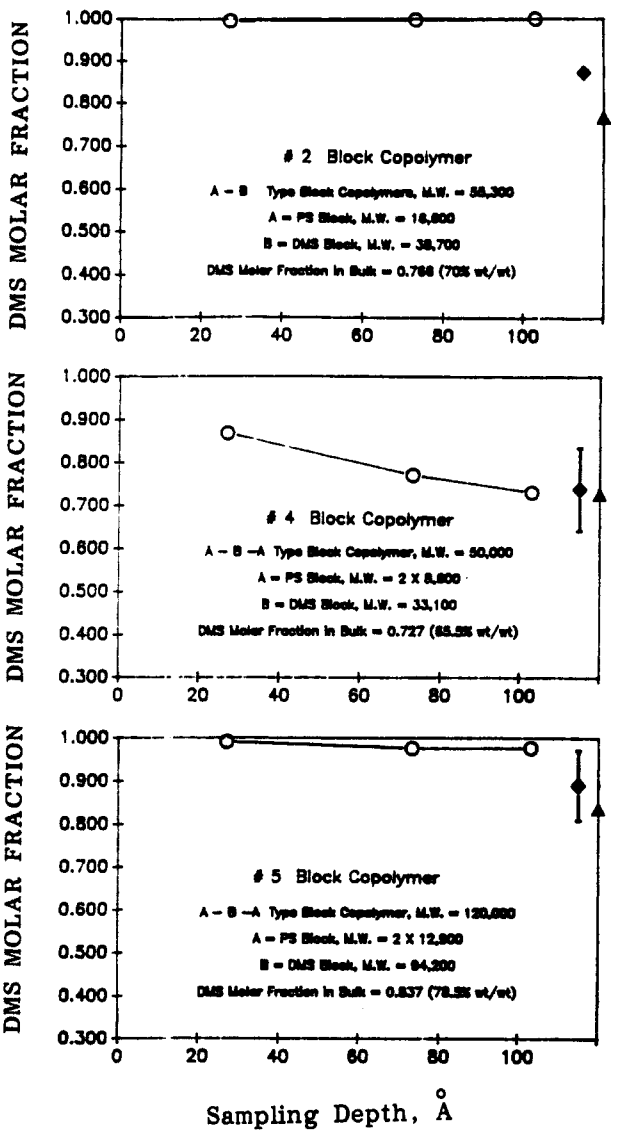

Figure 7. Depth profiles of the DMS molar fractions from both ESCA and ATR-FTIR for samples 2 of the PS–PDMS-type and 4 and 5 of PS–PDMS–PS-type block copolymers. Filled triangles are for the bulk DMS molar fractions, filled diamonds are for the DMS molar fractions from ATR-FTIR, and circles are for the DMS molar fractions from ESCA of the three samples. The profiles of samples 2, 4, and 5 are arranged from top to bottom.

In the case of BAB-type triblock copolymers (Figure 6, bottom), both samples have their PDMS concentration in the ATR-FTIR sampling region very close to their bulk concentration. The surface segregation effect of PDMS also disappears in the region sampled by ATR-FTIR.

Effect of the Architecture of Block Copolymers on PDMS Surface Segregation. The effect of the architecture of block copolymers on PDMS surface segregation is compared in Figure 7. Sample 2 (on the top) is a PS–PDMS diblock copolymer, and both samples 4 (in the middle) and 5 (on the bottom) are PS–PDMS–PS triblock copolymers. The PDMS block length of sample 2 (M_n = 38 700) is close to that of sample 4 (M_n = 33 100), and about half of that of sample 5 (M_n = 94 200). All three samples have comparable bulk PDMS concentrations (from 0.727 to 0.837 in DMS molar fraction). Pure PDMS consists the top layer of sample 2 within the ESCA sampling depth (up to 103 Å). But sample 4 with nearly the same PDMS block length and total molecular weight has a much lower PDMS surface concentration, and the DMS molar fraction decreases very quickly as the bulk is approached. Even in the outermost 27-Å region, sample 4 exhibits moderate PS presence (PS molar fraction 0.13). The PDMS surface segregation effect is no longer observed when the sampling depth is 103 Å. The difference of PDMS surface segregation between sample 2 and sample 4 indicates that the PDMS block length is not the only factor in determining the surface enrichment of the lower surface energy constant. However, sample 5 of the PS–PDMS–PS-type block copolymer, which has its PDMS block length twice as long as that of sample 2, shows a depth profile identical (within measurement errors) with that of sample 2 in all the surface regions sampled by ESCA and ATR-FTIR. The result means that a triblock copolymer of the ABA-type, with the lower surface energy component B block, needs to have the B block length about twice as long as that of an AB-type diblock copolymer to achieve the same surface segregation effect of an AB-type block copolymer with a similar composition.

Effect of Annealing on PDMS Surface Segregation of Block Copolymers. ESCA and ATR-FTIR results of annealed PS–DMS block copolymers are summarized in Table IV.

For AB diblock copolymers (nos. 1 and 3), there is no change in the PDMS concentration measured by ESCA after annealing. In the surface region sampled by ATR-FTIR, however, the PDMS concentration drops to its bulk

Table IV
DMS Molar Fraction at the Surface[a] and in the Bulk of PS–PDMS Block Copolymers after Annealing[c]

sample	15° [b]	45° [b]	90° [b]	ATR-FTIR	bulk
1	0.997 ± 0.032	0.990 ± 0.005	0.980 ± 0.011	0.866 ± 0.062	0.829
3	0.995 ± 0.022	0.995 ± 0.006	0.982 ± 0.005	0.815 ± 0.082	0.664
6	0.976 ± 0.079	0.988 ± 0.008	0.973 ± 0.012	0.704 ± 0.071	0.759
7	1.008 ± 0.044	1.014 ± 0.042	0.975 ± 0.017	0.762 ± 0.053	0.808
8	0.987 ± 0.015	0.931 ± 0.013	0.901 ± 0.011	0.883 ± 0.074	0.849
9	0.815 ± 0.007	0.645 ± 0.049	0.566 ± 0.017	0.263 ± 0.058	0.319

[a] ESCA data of different angles were calculated from C(1s)/Si(2p) atomic ratios. [b] ESCA take-off angles. [c] Samples were annealed at 140 °C for 3 days.

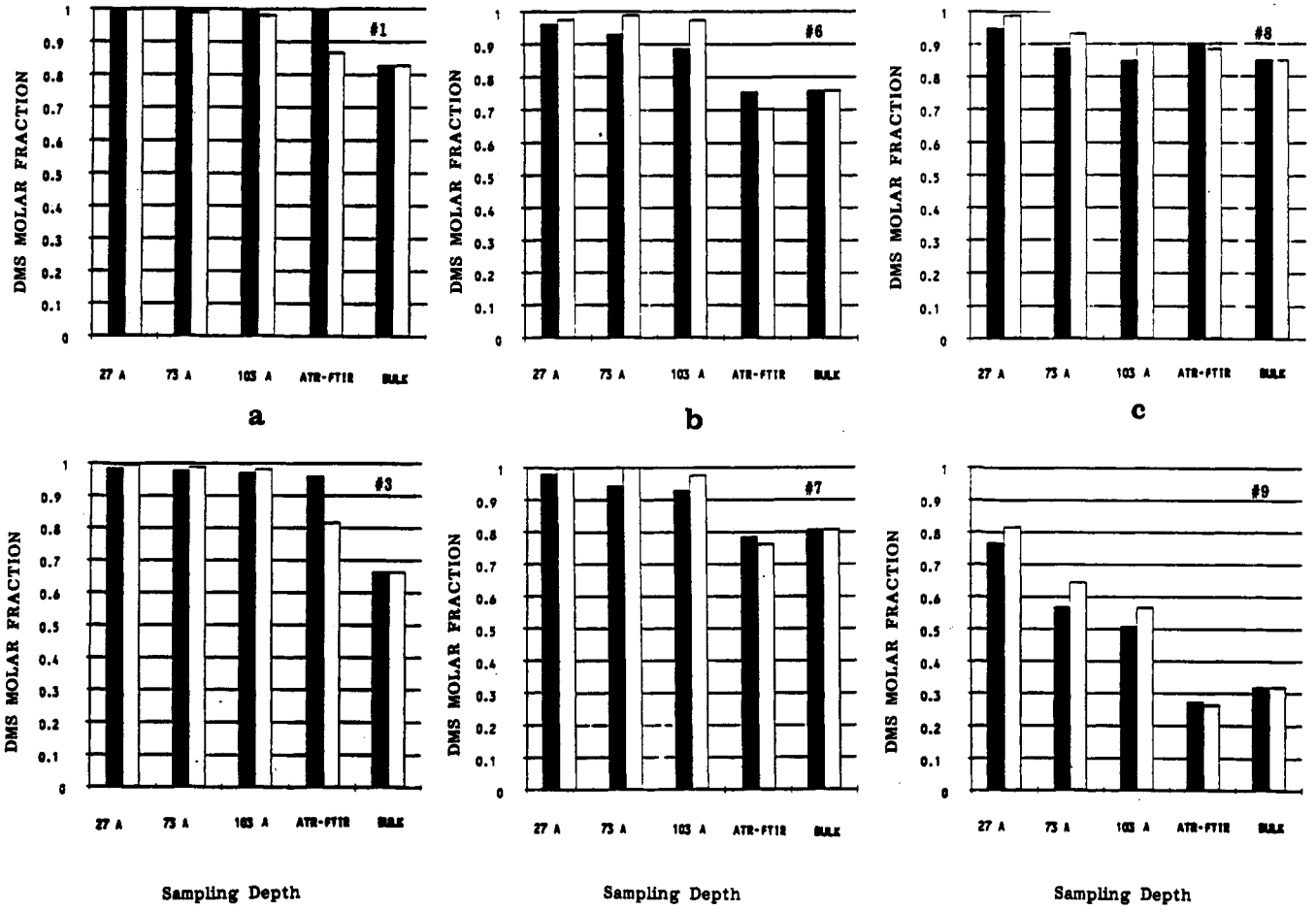

Figure 8. (a) PDMS surface concentrations of as-cast films (filled bars) and annealed films (hollow bars) of PS–PDMS diblock copolymers (samples 1 and 3). (b) PDMS surface concentrations of as-cast films (filled bars) and annealed films (hollow bars) of PS–PDMS–PS triblock copolymers (samples 6 and 7). (c) PDMS surface concentrations of as-cast (filled bars) and annealed films (hollow bars) of PDMS–PS–PDMS triblock copolymers (samples 8 and 9).

composition for sample 1, which has a relatively high PDMS bulk concentration, and is substantially lower than the PDMS concentration of the as-cast sample for sample 3 after annealing. The comparisons of the surface concentration of PDMS are illustrated in Figure 8a.

Samples 6 and 7 were annealed to determine the annealing effect on the PDMS surface segregation for the PS–PDMS–PS-type triblock copolymers (Figure 8b). No change within the measurement errors in the PDMS concentration measured by both ESCA and ATR-FTIR was found for sample 7, the one with a relatively longer PDMS block and higher PDMS bulk concentration. The ESCA results of sample 6 reveal that the outermost pure PDMS layer becomes thicker after annealing because the surface region measured by ESCA with a 90° take-off angle is composed of nearly 100% of PDMS for the annealed sample and about 90% of PDMS for the as-cast sample. The results indicate that annealing of the block copolymer samples promotes the surface segregation of PDMS, the lower surface energy component of the block copolymers.

The ESCA measurements of samples 8 and 9 of the PDMS–PS–PDMS-type triblock copolymers further demonstrate the annealing effect on the surface segregation of PDMS of the block copolymers. The PDMS concentrations, measured in all the ESCA sampling regions, of the annealed films of both samples 8 and 9 are higher than the corresponding PDMS concentrations of the as-cast films (Figure 8c).

Discussion

A PDMS segment, composed of $-Si(CH_3)_2O-$ repeat units, is relatively soft and flexible, and has a very low surface energy (20.4 mN/m at 20 °C). In contrast, a PS segment, with benzene rings attached to its backbone chain, is hard and rigid, and has a much higher surface energy (40.7 mN/m at 20 °C).[26] Chloroform is a common solvent for both PDMS and PS. The Flory–Huggins polymer–solvent interaction parameter χ at 20 °C for PDMS in chloroform solution is 0.5 when the PDMS concentration is low (0–20%), and 0.6 when the PDMS

concentration is very high (80–100%). The χ value at 20 °C for PS in chloroform solution is 0.5, which is the same as that for PDMS when the PDMS concentration is low (0–20%). Unlike the χ of PDMS, which increases as the polymer concentration increases, the χ of PS drops to 0.2 when the PS concentration in the chloroform solution is very high (60–100%).[27]

When a PS–PDMS block copolymer chloroform solution of a low polymer concentration is prepared, both PS and PDMS components in the block copolymer are well solubilized in the solution. The polymer concentration in the solution increases as the solvent evaporates. According to the relationship between the polymer–solvent interaction parameters and the polymer concentration, the PDMS blocks in the block copolymers become less soluble as the polymer concentration increases, but the PS blocks in the block copolymers become more soluble as the polymer concentration increases. Chloroform preferentially solubilizes the PS blocks of the PS–PDMS block copolymers in high polymer concentrations. As a result of the solubility differences, PDMS blocks separate from the PS blocks and spontaneously assembly themselves to an ordered array. The ordered morphological structures in concentrated block copolymer solutions have been confirmed by light scattering experiments.[28]

For a concentrated multicomponent polymer solution, the interactions between the polymer components are more important than the polymer–solvent interactions. The polymer–polymer interaction parameter χ_{ij} is approximately proportional to the square of the difference of the Hildebrand solubility parameters δ_i and δ_j for polymer component i and polymer component j, based on the Laar–Hildebrand equation. Since χ_{ij} is the measurement of the mixing enthalpy of polymers, the polymer mixture is predicted to separate when δ_i is much different from δ_j. The Hildebrand solubility parameters δ are 15.5 $MPa^{1/2}$ for PDMS and 18.5 $MPa^{1/2}$ for PS.[27] The solubility parameter difference of the two blocks in the PS–PDMS block copolymers is significant. A phase-separated morphology of the block copolymers should thus be expected.

Because of the large differences in surface energy and the large mixing enthalpy of the two different blocks of the PS–PDMS copolymers, PDMS blocks prefer to segregate to the free surface and form a PDMS microdomain, and leave PS blocks to form a microdomain next to the outermost pure PDMS layer to satisfy the thermodynamic requirement to minimize the total free energy of the block copolymer system. Lamellar models of arrangements of the two blocks, accordingly, are proposed and illustrated in Figure 9.

Figure 9, top, depicts the lamellar morphology model of the arrangement of the two different blocks of PS–PDMS diblock copolymers. The PDMS block in this block architecture has one free end and has the other end connected to a PS block. The free ends of the PDMS blocks tend to stretch out to the surface region very close to the interface[29] in the pure (or dominated) PDMS outermost layer. The PS blocks connected with the PDMS blocks in the outermost layer segregate to form a domain (or domains) adjacent to the first PDMS layer. In this PS domain, there should exist PS blocks connected with PDMS blocks in the second layer as well. The longer the PDMS block is, the larger volume this block can occupy in the first pure PDMS layer, and the thicker the first pure PDMS layer should be, according to this model.

But the situation for the ABA-type PS–PDMS–PS triblock copolymers with the PDMS block in the middle is diffferent.[4] Both ends of the PDMS blocks are

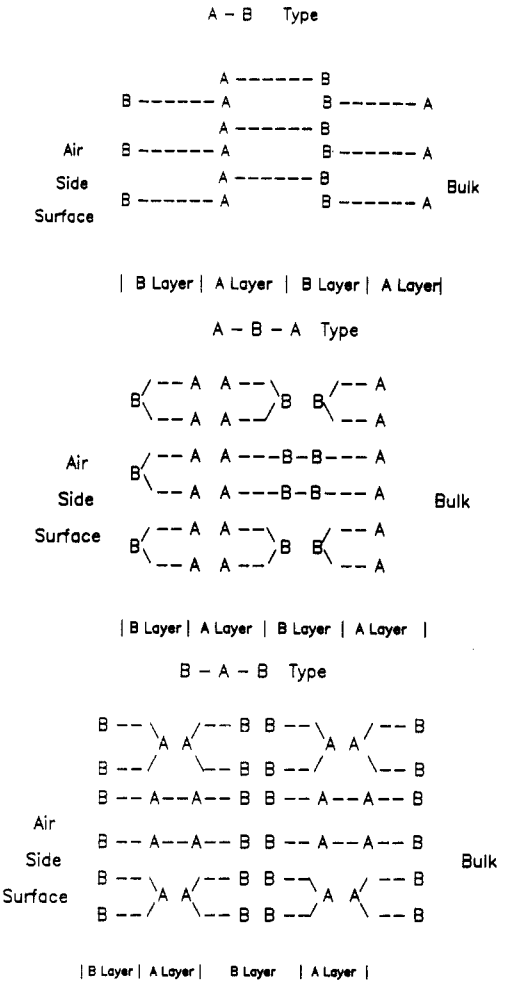

Figure 9. (Top) Arrangement of PDMS and PS blocks of PS–PDMS diblock copolymers on the air side surface based on a lamellar morphology. A and B represent PS and PDMS blocks, respectively. (Middle) Arrangement of PDMS and PS blocks in PS–PDMS–PS-type triblock copolymers on the air side surface based on a lamellar morphology. A and B represent PS and PDMS blocks, respectively. (Bottom) Arrangement of PDMS and PS blocks in PDMS–PS–PDMS-type triblock copolymers on the air side surface based on lamellar morphology. A and B represent PS and PDMS blocks, respectively.

constrained by the PS blocks, and there is no free end of the PDMS blocks. Each of the PS blocks has one connected end and one free end. For the same reason as in the AB-type block copolymers, PDMS blocks attempt to segregate to the free surface to form a PDMS microdomain. Having the PS block constraint applied on them, the PDMS block chains which exist in the outermost pure PDMS layer have to be bent over. The surface region very close to the interface, therefore, should be composed of the middle segments of the PDMS blocks as shown in Figure 9, middle. This bending effect of the PDMS block chains in the ABA-type block copolymers may account for the fact demonstrated here that the outermost pure PDMS layer of an ABA-type triblock copolymer has approximately the same thickness as that of an ABA-type diblock copolymer with about $^1/_2$ the PDMS block length. In the second PDMS block dominated layer, PDMS blocks can either spread out or bend over. So the architecture effect of the block copolymers on their morphology is more important in the very surface region than in the deeper region.

A lamellar surface morphology model for the BAB-type PDMS–PS–PDMS triblock copolymers is shown in Figure 9, bottom. For a PDMS–PS–PDMS block copolymer chain, each PDMS block has one free end and one

connected end with a PS block, as a PDMS block in an AB-type diblock copolymer does. All PDMS blocks of the PS–PDMS diblock copolymer chains present in the outermost surface region have to be present in the outermost PDMS layer. The PDMS blocks of the PDMS–PS–PDMS-type triblock copolymer chains present in the same outermost surface region, however, have two arrangement choices, either to have one PDMS block in the first PDMS dominated layer and the other PDMS block on the same copolymer chain in the second PDMS dominated layer or to have both PDMS blocks on the same copolymer chain in the outermost PDMS dominated layer. The PS blocks in the PS dominated layer could bend over or stretch out, depending on whether the two PDMS blocks on the same copolymer chain are in the same domain or not. Obviously, the thickness of the outermost PDMS dominated layer is dependent on the PDMS block length.

Theodorou[29] studied polymer melt surfaces by using a variable-density lattice model based on the thermodynamic concept of availability. For a free surface of a macromolecular liquid (such as monodisperse poly(dimethylsiloxane)homopolymer with MW = 3720, or 50 repeat units), the treatment revealed that PDMS density profiles in the free surface region of PDMS are sigmoidal, rising from a value of practially zero first to their asymptotic bulk value over a distance of about 15 Å. The thickness of the surface region, over which PDMS density variations are observed, is quite insensitive to both chain length and temperature. Bond orientation in this sparsely PDMS segment populated surface region was also found in higher oriented order than that in the deeper region (beyond 15 Å from the interface). Of the most interest is the result obtained concerning chain shape in the region near the free surface. In this highly attenuated surface region, PDMS chain coils are very narrow (or elongated in the direction normal to the free surface). The chains become pronouncedly flattened as one moves into the region of appreciable density. Deeper in the fluid PDMS phase, the flattening disappears gradually, as conformations relax to their unperturbed bulk dimensions as they are in solution. The length, over which this flattening effect disappears, is larger in the higher molecular weight system. The distributions of chain ends and middle segments were calculated. The surface enhancement in chain ends actually becomes dramatic for the high molecular weight PDMS. In the case of PDMS with 50 repeat units (MW = 3720), 51.5% of the total population of the outermost layer consists of the PDMS chain ends, even though the end segments represent only 0.8% of the total polymer mass. The PDMS surface morphology could be best summarized, according to this model, as one in which the topmost 15-Å sparsely populated layer is mainly composed of PDMS chain ends oriented perpendicular to the surface. This is followed by an intermediate layer with a PDMS chain flattened in the plane parallel to the free surface. The flattened layer is about 10 Å for PDMS with 50 segments and is larger when the number of segments of PDMS is larger. Finally there is the isotropic layer in which the PDMS chain dimension can be well described by Flory's root mean squared end-to-end length for unperturbed chains, $\langle r^2\rangle_0^{1/2}$, which is proportional to the square root of the number of repeat units of the PDMS chain, $N^{1/2}$.

On the polymer melt–solid interface side, the polymer melt surface morphology is different from that on the free surface side. There is no attenuated outermost surface layer. The variations in density are also weaker. Near a strongly adsorbing smooth solid surface, the liquid PDMS chains are pronouncedly flattened and densely packed. The average width of chains drops monotonically to its unperturbed value as one moves away from the solid, over a distance roughly equal to the end-to-end length. Subtle changes in density and local density are observed upon varying the strength of PDMS chain–solid interactions.

The surface morphology of PDMS obtained by the variable-density lattice treatment for the PDMS liquid on the free surface side could apply to our PS-PDMS block copolymer systems on the basis of two considerations. First, the outermost free surface region of the PS-PDMS block copolymers consists of a pure PDMS layer if the length of the PDMS blocks is sufficient and the bulk PDMS concentration is high, as shown in our studies by ESCA. Second, the phase of the PDMS blocks on our block copolymers is in the liquid state at room temperature. Whether the treatment on the polymer melt–solid side applies to this system requires further discussion, because the PDMS ends in the PDMS–PS microdomain interface region are mainly connected with PS blocks for AB-, ABA-, and BAB-type block copolymers, especially for ABA-type triblock copolymers which have no free PDMS block ends. The detailed morphology of the interface of the first pure PDMS layer–PS layer has to be examined.

Russell et al.[13] used neutron reflectivity to study symmetric PS–PMMA diblock copolymers. Their results showed a lamellar morphology with the lower surface energy component PS in the outermost surface region. Between the PS dominated layer and the PMMA dominated adjacent layer, there exists a layer, which was called the interface, composed of both components. The thickness of the interface, independent of the block length, was calculated to be 50 ± 3 Å. However, the volume fractions (or thickness) of the pure PS and pure PMMA domain (or layer) are dependent on the block chain length. Since the difference in surface energy between PS and PDMS is much larger than that between PS and PMMA, a narrower interface for a PS–PMMS block copolymer would be expected.

By adopting the above "interface" concept and applying the treatment using the variable-density lattice model for the polymer melt–solid interface to our PS–PDMS block copolymer system, the morphology of the intermediate region of the first pure PDMS layer–PS layer in the PS–PDMS block copolymers could be predicted. In the interface, there exists both PDMS and PS segments. If the pure PS layer adjacent to the interface is considered as a solid phase (in fact the PS phas is in the glassy state at room temperature) and the pure PDMS layer is considered as a polymer melt phase, the interface of the polymer melt–solid is not sharply defined and also the solid surface is not smooth, because of the chemical connection of the two different block chains in the block copolymers. To have a better defined interface and smooth solid surface, both PDMS and PS chain ends should be flattened along the plane of the interface.[29,30] For PS–PDMS block copolymers, however, the connected segments at the connection of the two connected PDMS and PS blocks in the interface region should orient perpendicular to the interface. This orientation of the connected block ends increases the interface width. Hence, the interface width, or volume fraction of the interface, is related to the fraction of connected block ends in the interfacial region.

The ratio of free block ends to connected block ends differs in block copolymer architectures. There are a total of six block ends of both PDMS and PS blocks on each polymer chain for both ABA- and BAB-type triblock copolymers. But four out of the six block ends, or two-

thirds, are connected ends. While there are a total of four block ends of both PDMS and PS blocks on each polymer chain for AB-type diblock copolymers, only half of the block ends are connected. The fraction of connected block ends of triblock copolymers is larger than that of diblock copolymers, which means that triblock copolymers should have a larger interface fraction and relatively thinner pure PDMS outermost layer than diblock copolymers. This effect has been observed in our experiments. The results show that the diblock copolymers have the thickest outermost pure PDMS layer among the three types of block copolymers studied.

Therefore, PDMS block chains in the interface of the PS–PDMS block copolymers must not have been as well flattened as chains of a PDMS homopolymer would be in a smooth solid interface. Because there exists the enhancement of PDMS block ends in the interface, more connected ends of PDMS blocks in the PS–PDMS block copolymers may be present in the interface region as the PDMS component than stay in the inner region of PDMS microdomains. The PS blocks in their glassy state have a flattening effect of the backbones in the interface region[30] and keep their ends flatly laid in the interface as the PS component. The connected PDMS block ends protruding into the interface region act as "roots" in a PS-rich domain for the PDMS segments remaining in the pure PDMS domains. These roots may account for the many desirable mechanical and adhesive properties of block copolymers over simply mixed polymer blends, which usually have sharply divided interfaces between different domains.

Annealing an as-cast block copolymer sample may change the morphology of the block copolymer in two ways, promoting segregation and affecting morphology orientation. The effect of promoting segregation is exemplified by the PDMS concentration increase in the surface regions probed by ESCA after annealing the as-cast samples for samples 6, 8, and 9. The PDMS concentration decreases in the surface region probed by ATR-FTIR after annealing the as-cast samples for samples 1 and 3 may be attributed to the morphology orientation change.

Conclusions

The outermost surface region (up to 27 Å) of the PS–PDMS block copolymers of all AB, ABA, and BAB types is composed of the nearly pure PDMS component if the DMS molar fraction in the bulk is high (>0.6). For the block copolymers with a low DMS molar fraction in the bulk (<0.5), the segregation of PDMS in the same surface region is still very high, but a substantial amount of the PS component is present in this layer also.

In a wider surface region (0–100 Å) there exist either only PDMS blocks or both PDMS and PS blocks, depending on the block architecture, block length, and bulk DMS molar fraction. Among these three features, the block architecture and block length have more important effects on the surface morphology of the block copolymers. AB-type PS–PDMS diblock copolymers are easier to have higher surface segregation of the PDMS blocks and have a thicker PDMS dominated layer than ABA- and BAB-type block copolymers of the similar bulk composition and PDMS block length.

In the surface region probed by the ATR-FTIR measurements, the PDMS concentration of both ABA- and BAB-type triblock copolymers is equal to or near the bulk PDMS concentration. However, the PDMS concentration in this region could still be higher than the bulk PDMS concentration even after annealing the as-cast samples for AB diblock copolymers when the PDMS block is long enough.

Acknowledgment. The authors would like to thank Dr. Dale J. Meier of Michigan Molecular Institute (Midland, MI) for his generous donation of the PS–PDMS block copolymers. This work was supported by the National Science Foundation, Division of Materials Research (Polymers Program), Grant No. 8720650. Dr. Terrence G. Vargo's help in setting up the ATR-FTIR experiments is also greatly appreciated.

References and Notes

(1) See, for example: Bates, F. S. *Science* **1991**, *251*, 898 and references therein.
(2) Noshay, A.; McGrath, J. E. *Block Copolymers: Overview and Critical Survey*; Academic Press: New York, 1977.
(3) Schmitt, R. C.; Gardella, J. A., Jr.; Magill, J. H.; Chin, R. L. *Polymer* **1987**, *28*, 1462.
(4) Helfand, E. and Wasserman, Z. R. *Macromolecules* **1976**, *9*, 879.
(5) Clark, D. T.; Peeling, J.; O'Malley, J. M. *J. Polym. Sci., Polym. Chem. Ed.* **1976**, *14*, 543.
(6) Bajaj, P.; Varshney, S. K. *Polymer* **1980**, *21*, 201.
(7) Hasegawa, H.; Hashimoto, T. *Macromolecules* **1985**, *18*, 589.
(8) Hartney, M. A.; Novembre, A. E.; Bates, S. E. *J. Vac. Sci. Technol.* **1985**, *B3* (5), 1346.
(9) Vargo, T. G.; Gardella, J. A., Jr. *J. Vac. Sci. Technol.* **1989**, *A7* (3), 1733.
(10) (a) Green, P. F.; Christensen, T. M.; Russell, T. P.; Jerome, R. *J. Chem. Phys.* **1990**, *92*, 1478. (b) Green, P. F.; Christensen, T. M.; Russell, T. P. *Macromolecules* **1991**, *24*, 252.
(11) Schmitt, R. L.; Gardella, J. A., Jr.; Magill, J. H.; Salvati, L., Jr.; Chin, R. L. *Macromolecules* **1985**, *18*, 2675.
(12) Coulon, G.; Russell, T. P.; Deline, V. R.; Green, P. F. *Macromolecules* **1989**, *22*, 2581.
(13) Anastasiadis, S. H.; Russell, T. P.; Satija, S. K.; Majkrzak, C. F. *J. Chem. Phys.* **1990**, *92*, 5677.
(14) Shull, K. R.; Winey, K. I.; Thomas, E. L.; Kramer, E. J. *Macromolecules* **1991**, *24*, 2748.
(15) Shull, K. R.; Kramer, E. J.; Hadziioannou, G.; Tang, W. *Macromolecules* **1990**, *23*, 4780.
(16) Green, P. F.; Christensen, T. M.; Russell, T. P.; Jerome, R. *Macromolecules* **1989**, *22*, 2189.
(17) Mittlefehldt, E. R.; Gardella, J. A., Jr. *Appl. Spectrosc.* **1989**, *43*, 1172.
(18) Hook, J. T.; Gardella, J. A., Jr.; Salvati, L., Jr. *J. Mater. Res.* **1987**, *2* (1), 132.
(19) McGrath, J. E.; Dwight, D. W.; Riffle, J. S.; Davison, T. F.; Webster, D. C.; Viswanathan, R. *Polym. Prepr. (Am. Chem. Soc., Div. Polym. Chem.)* **1979**, *20*, 528.
(20) Thomas, H. R.; O'Malley, J. J. *Macromolecules* **1979**, *12*, 322.
(21) Thomas, H. R.; O'Malley, J. J. *Macromolecules* **1981**, *14*, 1316.
(22) Fredrickson, G. H. *Macromolecules* **1987**, *20*, 2535.
(23) Chen, X.; Gardella, J. A., Jr.; Kumler, P. L. *Macromolecules*, following paper in this issue.
(24) Harrick, N. J. *Internal Reflectance Spectroscopy*; John Wiley & Sons: New York, 1979; p 30.
(25) Brown, C. W.; Lynch, P. F.; Obremski, R. J.; Lavery, D. S. *Anal. Chem.* **1982**, *54*, 1472.
(26) Brandrup, J.; Immergut, E. H. *Polymer Handbook*, 3rd ed.; John Wiley & Sons: New York, 1989.
(27) Barton, F. M. *Handbook of Polymer-Liquid Interaction Parameters and Solubility Parameters*; CRC Press, Inc.: Boca Raton, FL, 1990.
(28) Balsara, N. P.; Stepanek, P.; Lodge, T. P.; and Tirrell, M. *Macromolecules* **1991**, *24*, 6227.
(29) (a) Theodorou, D. N. *Macromolecules* **1989**, *22*, 4578. (b) Theodorou, D. N. *Macromolecules* **1989**, *22*, 4589.
(30) Mansfield, K. F.; Theodorou, D. N. *Macromolecules* **1990**, *23*, 4430.